

## Measurement of Quenching Factor for Nuclear Recoils in CsI(Tl) Crystal \*

YUE Qian<sup>1,1)</sup> LI Jin<sup>1</sup> LIU Yan<sup>1</sup> LI Hao-Bin<sup>2,3</sup> WONG H. T.<sup>2</sup> WONAG M. Z.<sup>3</sup>

1 (Institute of High Energy Physics, CAS, Beijing 100039)

2 (Institute of Physics, Academia Sinica, Taipei 11529)

3 (Department of Physics, Taiwan University, Taipei 10600)

**Abstract** Detection of dark matter using CsI(Tl) scintillating crystal as the detector has gathered more and more interests. In this paper, the quenching factor of nuclear recoils induced by incident neutron beam was measured based on Pulse Shape Discrimination (PSD) method to identify events of nuclear recoils from background. It is shown that the quenching factor increases with the decreased recoil energy in the range of 7 keV to 132 keV. This result shows the great advantage of CsI(Tl) crystal detector in detecting of dark matter.

**Key words** CsI(Tl) crystal, neutron elastic scattering, dark matter, pulse shape discrimination

### 1 Introduction

There are more and more interests for physicists to study the nature of dark matter<sup>[1,2]</sup>. One of candidates of dark matter, weakly interacting massive particle (WIMP), has attracted many physicists to focus on its detection. Many experiments have obtained exciting results for the detection of dark matter<sup>[3,4]</sup>. In some experiments recoiled nuclei induced by incident neutron beam in a suitable detector were used to simulate the nuclei recoil of detector scattering off by WIMP particles and Pulse Shape Discrimination (PSD) method has been used to discriminate signals induced by nuclear recoils and gammas or electrons<sup>[5,6]</sup>. In this paper, we use the PSD method to analyse pulses of recoiled nuclei induced by 8 MeV neutron beam to derive the quenching factor of nuclear recoils in the energy range from 7 keV to 132 keV. The quenching mechanism is due to the less light yield of heavier nucleus comparing to that of electron with same energy. Here the quenching factor is defined as follows:

$$QF = \frac{E_r^e}{E_R} \quad (1)$$

where  $E_r^e$  is the electron-equivalent recoil energy of recoiled nucleus and  $E_R$  is theoretical recoil energy calculated from the energy of incident neutron and scattering angle of neutron.

### 2 Experimental Setup

The reaction  $D(d, n)^3\text{He}$  was used to obtain 8 MeV pulsed neutron beam. The pulsed deuteron

Received 7 November 2001

\* Supported by Science Foundation of Two Sides of Strait (19975050 and 89-N-FA01-1-4-2, 89-2112-M-001-056, 90-2112-M-001-037)

1) E-mail: yueq@mail.ihep.ac.cn

beam with an energy of 5.6 MeV was supplied by HI-13 Tandem accelerator at China Institute of Atomic Energy (CIAE), interacted with the deuterium gas target. A small CsI(Tl) crystal detector (3cm in diameter, 3cm long) was hit by the collimated neutron beam. The block diagram of experimental setup is shown as Fig.1. The arrangement of the CsI(Tl) crystal, neutron detector and the neutron collimator has been described in the Ref.[7].

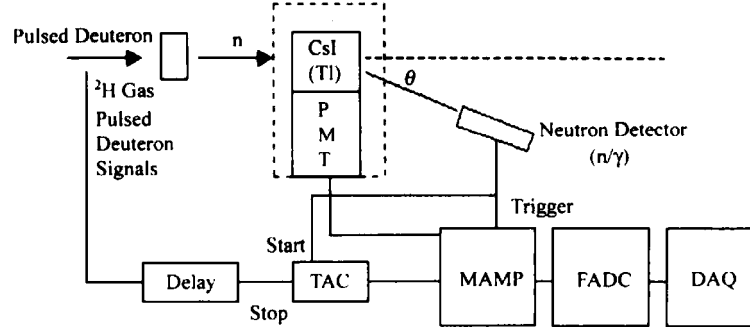


Fig.1. Block diagram of the experimental setup.

The incident neutrons were scattered off by cesium, iodine nuclei of the detector and proton, carbon nuclei which came from the black plastic tape and Teflon of the wrapping layer of CsI(Tl) crystal. The scattered neutron was detected by liquid scintillator (Co-261, ST-451) detectors, 105mm in diameter and 50mm in length, equipped with Photo-multiplier Tube (PMT, Philips XP-2041) readout and gave a trigger signal to the homemade Main Amplifier (MAMP). At the same time, the fluorescence of recoiled nuclei in CsI(Tl) crystal was collected by PMT (CR110, Hamamatsu Photonics, China) and the output current signal was passed to MAMP. The signal coming from the neutron detector was also used as the start signal of a Time-Of-Flight (TOF) system. The stop signal of TOF system came from the delayed pulsed deuteron beam. This TOF signal was also passed to MAMP and recorded for further neutron tagging. All of these signals passed to MAMP were digitized by home-made Flash Analog-to-Digital Converter (FADC) and recorded by a data acquisition system. The details of the electronics can be found in the Ref.[8].

The energies of recoiled nuclei can be decided by the scattering angles  $\theta$ , which were changed from  $20^\circ$  to  $95^\circ$ , and the recoil energy changed from 7 keV to 132 keV. The pulse shape recorded by FADC system has a pre-trigger and post-trigger period of  $5 \mu\text{s}$  and  $25 \mu\text{s}$ , respectively. For more details, one can see the Refs.[7,8].

### 3 Data Process and Results

The energy of recoiled nucleus being scattered by incident neutron was determined by the nuclear mass of detector and scattering angle  $\theta$ , and can be calculated out by a kinematical formula:

$$T = \frac{2A}{(1+A)^2} (1 - \cos\theta) E_n \quad (2)$$

where  $A$  is the mass of nucleus and  $E_n$  is the energy of incident neutron. The TOF of scattering neutron will be different at a special angle for the different nucleus and would be used to identify events induced by recoiled nuclei of cesium or iodine from that by proton, which is much lighter. The TOF spectrum at an angle  $95^\circ$  is displayed in Fig.2(a). On the platform of random coincidence, two peaks have been found and can be attributed to the neutron elastic scattering off by proton and some

heavier nuclei such as cesium, iodine and carbon, respectively. Because of the large scattering angle and relative light mass, proton-induced events were much less than that of heavier nuclei. For each signal of CsI(Tl) crystal, several parameters were used to describe the pulse shape. The first was  $A_{bin}$ , which is defined as the time bin where the amplitude of signal reached its maximum value. The other two were  $R$  and  $\langle t \rangle$  which were defined as follows:

$$\langle t \rangle = \frac{\sum_{i=1}^{50} (A_i t_i)}{\sum_{i=1}^{50} A_i}$$

and

$$\frac{\sum_{i=1}^{30} A_i}{\sum_{i=1}^{50} A_i} \quad (4)$$

where  $A_i$  is the FADC amplitude at a time bin  $t_i$ . All of these parameters at  $95^\circ$  have also been displayed in Figs. 2(b), (c) and (d). One can see the different parts for recoil signal and background in these three plots, respectively.

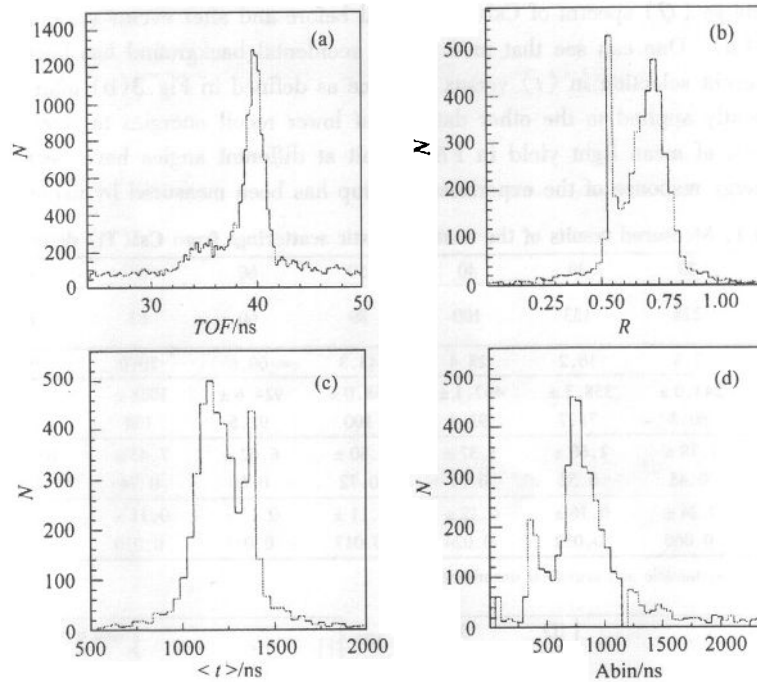


Fig. 2. The distribution of  $TOF$ ,  $\langle t \rangle$ ,  $R$  and  $A_{bin}$  for recoils and backgrounds at  $95^\circ$

The scattered plots for  $\langle t \rangle$  versus  $TOF$  as well as  $\langle t \rangle$  versus  $R$  for the data set at  $95^\circ$  are shown in Figs. 3(a) and (b), respectively. There are clear separations between the Cs or I nuclear recoil events, represented by the box region, and the accidental background events caused by the recoils of the wrapping materials (protons as well as other heavy nuclei such as carbon) and from environments. In Fig. 3(a), all the events relative at scattering angle  $95^\circ$  are shown. We first use the parameter  $TOF$  to make the event selection and require it is greater than 38.5 ns and less than

42 ns. All the event after this criterion of selection are shown in Fig. 3(b). We used the cut box displayed in the Fig. 3(b) as a selection criterion to get the events of recoil after cutting for parameter  $Abin$  which is great than 500 ns and less than 1500 ns (see Fig. 2(d)).

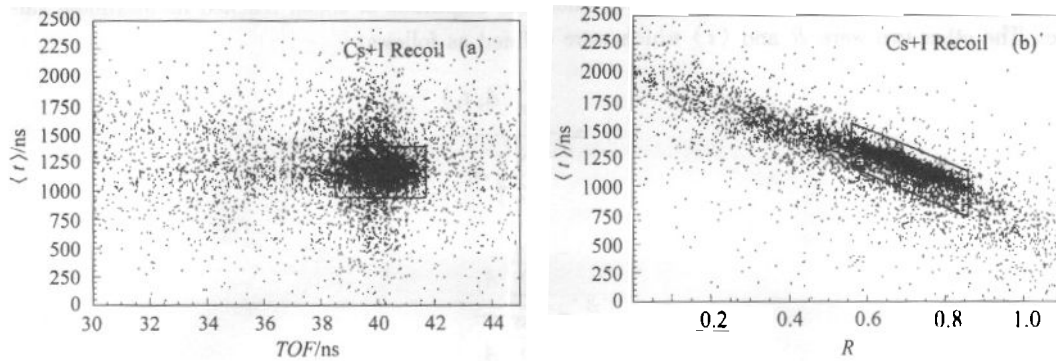


Fig.3. Scattered plots for the  $\langle t \rangle$  parameter versus the  $TOF$  values and  $R$  parameters for the nuclear recoil events at  $95^\circ$ . The box region represents the CsI nuclear recoil events, indicating clear separations from the accidental backgrounds.

The total charge ( $Q$ ) spectra of CsI(Tl) crystal before and after events selection are shown in Figs. 4(a) and (b). One can see that most of the accidental background has been rejected. The same method of event selection in  $\langle t \rangle$  versus  $R$  space as defined in Fig. 3(b) after  $TOF$  and  $Abin$  cuts are subsequently applied to the other data set at lower recoil energies to select nuclear recoil events. The results of mean light yield in FADC unit at different angles have been summarized in Table 1. The energy response of the experimental setup has been measured by using  $\gamma$  sources such

Table 1. Measured results of the neutron elastic scatterings from CsI(Tl) detector.

Angle/ $^\circ$	20	30	40	50	60	65	80	95
Neutron Detector Distance/cm	228	133	100	89	60	63	70	68
Recoil Energy/keV	7.3	16.2	28.4	43.3	60.6	70.0	100	132
Mean Light Output (FADC Unit)	$243.0 \pm 60.8$	$358.3 \pm 71.7$	$467.1 \pm 93.4$	$668.0 \pm 100$	$924.6 \pm 92.5$	$1038 \pm 104$	$1411 \pm 141$	$1869 \pm 187$
Electron-Equivalent Light Yield/keV	$1.78 \pm 0.45$	$2.60 \pm 0.52$	$3.37 \pm 0.67$	$4.80 \pm 0.72$	$6.62 \pm 0.66$	$7.43 \pm 0.74$	$10.1 \pm 1.0$	$13.3 \pm 1.3$
Quenching Factor	$0.24 \pm 0.060$	$0.16 \pm 0.032$	$0.12 \pm 0.024$	$0.11 \pm 0.017$	$0.11 \pm 0.011$	$0.11 \pm 0.010$	$0.10 \pm 0.010$	$0.10 \pm 0.010$

Errors are combined systematic and statistical uncertainties.

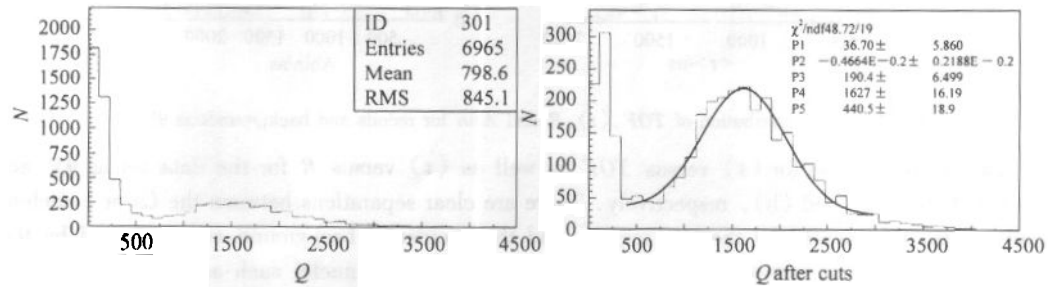


Fig.4. The energy spectra at angle  $95^\circ$  before cuts (top) and after cuts (down).

as  $^{109}\text{Cd}$  and  $^{133}\text{Ba}^{9-}$ . The electron-equivalent energies of recoiled nuclei were also shown in this table. The measured quenching factors are shown in Fig.5.

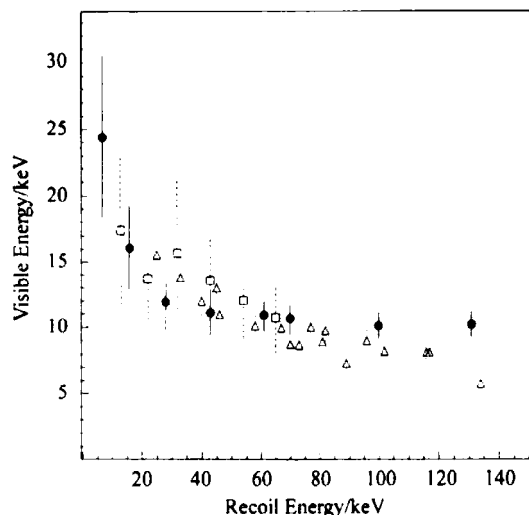


Fig.5. The quenching factors measured in this work (solid circle). Open squares are from Ref. [10], and open triangles are from Ref. [11].

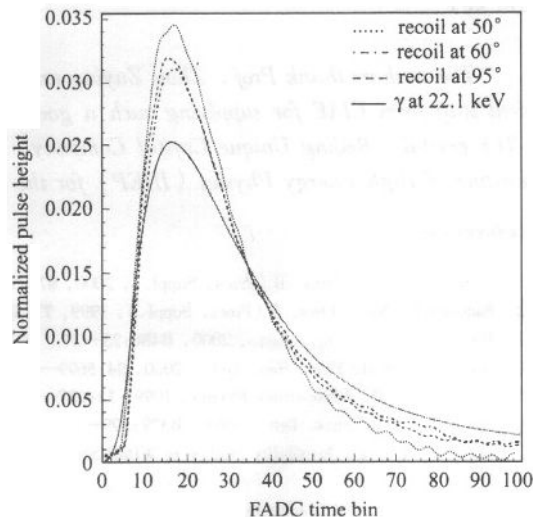


Fig.6. The pulse shapes of nuclear recoils at different angles and  $\gamma$ -ray at 22.1 keV. All the pulses have been normalized by their total charges.

The uncertainties of light yield and quenching factor at different angles have also been shown in Table 1. This uncertainty mainly comes from three parts. The first is from statistical error and is usually less than 3%. The second part is from the correction of light yield. The integration time for current signal to get the total charge was chosen as 50 FADC time bins for all the scattering angle of neutron. One can see from Fig.6 that 50 FADC time bins of integration make partly loss of the total charge of the recoil event. We change the integration time for events of angle  $95^\circ$  from 50 to 120 FADC time bins and get a correction factor 1.15 for the total charge. The error of this correction factor is about 5% for all angles. Another uncertainty comes from the selection of the border of cut box as shown in Fig.3. This is the main contribution of the error and increases with the recoil energy decreasing. The error bars have also been plotted in the Fig.5. There is a clear increase of quenching factor when the recoil energy decreases. This trend has also been found by several experiments<sup>[10,11]</sup>.

Several pulses for different angles and 22.1 keV  $\gamma$ -ray have been depicted in Fig.6. All the pulses have been normalized by their total charges. The pulse difference between recoil nuclei and  $\gamma$ -ray has been shown and there are almost same pulse shapes for the recoiled nuclei in different energies. It can be seen that pulses of heavier nuclei have relatively smaller decay time than that of  $\gamma$ s.

#### 4 Summary

In this paper, a measurement of the quenching factor of cesium and iodine nuclei in a CsI(Tl) crystal is presented. This measurement is based on Pulse Shape Discrimination (PSD) method. The cut conditions in this experiment are effective enough to reject background from events of recoil when

energy is great than 4 keV and become less effective when energy is low. A trend of increasing quenching factor with decreasing recoil energy has been obtained in the energy range from 7 keV to 132 keV.

*The authors thank Prof. Zhou Zuying and Tang Hongqing for the helpful discussions and technical staff from CIAE for supplying such a good neutron beam. We also thank the producer of CsI (TI) crystal, Beijing Unique Crystal Company. Thanks are also given to some technical persons of Institute of High Energy Physics (IHEP) for the transportation of the experimental setup.*

## References

- 1 Morales A. Nucl. Phys. B (Procs. Suppl.), 2000, **87**:477—488
- 2 Sadoulet B. Nucl. Phys. B (Procs. Suppl.), 1999, **77**:389—397
- 3 Bernabei R et al. Phys. Lett., 2000, **B480**:23—31
- 4 Abusaidi R et al. Phys. Rev. Lett., 2000, **84**:5699—5703
- 5 Gerbier C et al. Astroparticle Physics, 1999, **11**:287—302
- 6 Smith P T et al. Phys. Lett., 1996, **B379**:299—308
- 7 WANG M Z et al. Feasibility Studies of WIMP Searches with CsI (TI) Scintillating Crystals Nu-ex/200110003, Submitted to Phys. Rev. C
- 8 LAI W P et al. Nucl. Instrum. Meth., 2001, **A465**:550—565
- 9 YUE Qian et al. HEP & NP, 2002, **26**(7):728(in Chinese)  
(岳骞等. 高能物理与核物理, 2002, **26**(7):728)
- 10 Kudryavtsev V A et al. Nucl. Instrum. Methods, 2001, **A456**:272—279
- 11 Pecourt S et al. Astroparticle Physics, 1999, **11**:457—462

## CsI(Tl)晶体中反冲 Cs 和 I 核 Quenching Factor 的测量

岳骞<sup>1;1)</sup> 李金<sup>1</sup> 刘延<sup>1</sup> 李浩斌<sup>2,3</sup> 王子敬<sup>2</sup> 王名儒<sup>3</sup>

1(中国科学院高能物理研究所 北京 100039)

2(中研院物理研究所 台北 11529)

3(台湾大学物理系 台北 10600)

**摘要** 许多实验对用 CsI(Tl) 闪烁晶体作为探测器来寻找和探测暗物质的可行性进行了研究. 本工作利用 8MeV 单能中子轰击 CsI(Tl) 晶体探测器来研究 Cs 核和 I 核的 Quenching Factor. 在数据处理中, 运用脉冲形状甄别 (PSD) 方法来分辨反冲核信号和本底信号. 实验结果表明, 在 7keV 到 132keV 的能区中, Quenching Factor 随着反冲核能量的减少而增加. 在探测暗物质的实验中, 这一性质对于 CsI(Tl) 晶体探测器获得较低的能量阈值是很有利的.

**关键词** CsI(Tl) 晶体 中子弹性散射 暗物质 脉冲形状甄别

2001-11-07 收稿

\* 海峡两岸自然科学基金 (19975050 和 89-N-FA01-1-4-2, 89-2112-M-001-056, 90-2112-M-001-037) 共同资助

1) E-mail: yueq@mail.ihep.ac.cn